HHS Public Access

Author manuscript

Biol Psychiatry. Author manuscript; available in PMC 2024 September 01.

Published in final edited form as:

Biol Psychiatry. 2023 September 01; 94(5): 393–404. doi:10.1016/j.biopsych.2023.01.018.

Alcohol dependence modifies brain networks activated during withdrawal and reaccess: a c-fos-based analysis in mice

Alison V. Roland, Ph.D.[1,*], **Cesar A.O. Coelho, Ph.D.**[3,*], **Harold L. Haun, Ph.D.**[1], **Carol A. Gianessi, Ph.D.**[1], **Marcelo F. Lopez, Ph.D.**[7], **Shannon D'Ambrosio, B.S.**[1], **Samantha N. Machinski, B.A.**[1], **Christopher D. Kroenke, Ph.D.**[10,11,12], **Paul W. Frankland, Ph.D.**[3,4,5,6], **Howard C. Becker, Ph.D.**[7,8,9], **Thomas L. Kash, Ph.D.**[1,2]

[1.]Bowles Center for Alcohol Studies, University of North Carolina School of Medicine, Chapel Hill, NC, USA.

[2.]Department of Pharmacology, University of North Carolina School of Medicine, Chapel Hill, NC, USA.

[3.]Neuroscience and Mental Health, The Hospital for Sick Children, Toronto, ON, Canada

[4.]Dept. of Physiology, University of Toronto, Toronto, ON, Canada

[5.]Dept. of Psychology, University of Toronto, Toronto, ON, Canada

[6.]Institute of Medical Sciences, University of Toronto, Toronto, ON, Canada

[7.]Charleston Alcohol Research Center, Department of Psychiatry and Behavioral Sciences, Medical University of South Carolina, Charleston, SC

[8.]Department of Neuroscience, Medical University of South Carolina, Charleston, SC

[9.]Ralph H. Johnson Department of Veterans Affairs Medical Center, Charleston, SC

[10.]Division of Neuroscience, Oregon National Primate Research Center, Oregon Health & Science University, Beaverton, OR

[11.]Department of Behavioral Neuroscience, Oregon Health & Science University, Portland, OR

[12.]Advanced Imaging Research Center, Oregon Health & Science University, Portland, OR

Abstract

Background: High-level alcohol consumption causes neuroplastic changes in the brain that promote pathological drinking behavior. Some of these changes have been characterized in defined

Corresponding Author: Thomas Kash, Ph.D., CB 7178 Thurston Bowles Building, 104 Manning Drive, Chapel Hill, NC 27599, thomas_kash@med.unc.edu.

*These authors contributed equally to this work.

Conflicts of Interest

The authors report no biomedical financial interests or potential conflicts of interest.

brain circuits and cell types, but unbiased approaches are needed to explore broader patterns of adaptations.

Methods: We employed whole-brain c-fos mapping and network analysis to assess patterns of neuronal activity during alcohol withdrawal and following reaccess in a well-characterized model of alcohol dependence. Mice underwent four cycles of chronic intermittent ethanol (CIE) to increase voluntary alcohol consumption, and a subset underwent forced swim stress (FSS) to further escalate consumption. Brains were collected either 24 hours (withdrawal) or immediately following a one-hour period of alcohol reaccess. C-fos counts were obtained for 110 brain regions using iDISCO and ClearMap. We then classified mice as high or low drinkers (HD or LD) and used graph theory to identify changes in network properties associated with high-drinking behavior.

Results: During withdrawal, CIE mice displayed widespread increased c-fos expression relative to AIR mice, independent of FSS. Reaccess drinking reversed this increase. Network modularity, a measure of segregation into communities, was increased in HD mice after alcohol reaccess relative to withdrawal. The cortical amygdala (COA) showed increased cross-community coactivation during withdrawal in HD mice, and COA silencing in CIE mice reduced voluntary drinking.

Conclusions: Alcohol withdrawal in dependent mice causes changes in brain network organization that are attenuated by reaccess drinking. Olfactory brain regions, including COA, drive some of these changes and may play an important but underappreciated role in alcohol dependence.

Keywords

alcohol; chronic intermittent ethanol; mice; c-fos; networks; graph theory

Introduction

Alcohol use disorders (AUD) develop following long-term high-level alcohol consumption, which causes persistent molecular and cellular neuroadaptations across the brain (1,2). While initial alcohol use is motivated by its rewarding properties, pathological drinking is driven in part by negative affective and somatic symptoms that develop when alcohol is withdrawn. Alcohol-induced plasticity of stress systems is central to this transition, and altered stress responses may drive relapse drinking (1,2). This plasticity has been studied using rodent models, such as the chronic intermittent ethanol (CIE) vapor model of alcohol dependence (3). Although its effects are strain- and duration-dependent, CIE can evoke withdrawal-like symptoms in mice, including enhanced seizure susceptibility (4), locomotor changes (5), affective disturbances (6), and increased voluntary alcohol drinking (7,8). CIE-induced increases in drinking can be reliably escalated by administering forced swim stress (FSS) four hours prior to drinking (9–11), facilitating the study of stress-alcohol interactions.

While rodent models have generated important insight into key neurochemicals and circuits that contribute to alcohol dependence, existing studies are biased toward brain regions previously implicated in addiction (12). The recent implementation of unbiased whole-brain approaches and graph theory has begun to provide a broader perspective of alcohol's effects

on the brain (13). Network-based methods provide insight into how the brain produces complex cognitive states and behaviors, which arise from coordinated activity among communities of brain regions (14). A recent study employed single-cell whole-brain imaging and graph theory to assess the functional networks associated with alcohol abstinence in CIE mice (15). Relative to casual drinkers and alcohol-naïve mice, CIE mice displayed a decrease in network modularity after one week of abstinence, indicating that alcohol-induced plasticity is reflected in network-level changes. However, plasticity is dynamic across the cycle of intoxication, withdrawal, and relapse, and comparison of networks after voluntary reaccess drinking relative to withdrawal is important for discerning the mechanisms that drive relief drinking.

The present study used whole-brain c-fos mapping and graph theory to compare coactivation networks in mice during acute withdrawal and after reaccess drinking in a model of alcohol dependence. We used CIE/FSS mice to assess how stress modulates brain-wide activity patterns to escalate drinking, and examined c-fos expression at two time points: acute withdrawal (24h), and immediately following a 1h alcohol reaccess period. Using the iDISCO/ClearMap pipeline, we obtained c-fos-positive cell counts for 110 brain regions. We used interregional Pearson correlations to identify functional coactivation networks representing the neural state during withdrawal and reaccess in groups selected for low-drinking (LD) and high-drinking (HD) behavior. We compared global network properties between groups, and captured two community-based properties, within-community strength (wcs) and diversity (h), for each brain region. Several brain regions in HD mice during withdrawal showed high diversity that was normalized by reaccess drinking; due to their strong connectivity to many other regions, these regions are predicted to disproportionately influence network activity (14). Using a chemogenetic approach, we then targeted one of these regions, the cortical amygdala, to test the hypothesis that activity in high-diversity regions influences drinking behavior in CIE mice during withdrawal.

Materials and Methods

Materials and Methods are included in Supplemental Information.

Results

Chronic intermittent ethanol increased voluntary ethanol drinking

To explore the effects of alcohol dependence on brain-wide patterns of c-fos activation, we used the CIE/FSS paradigm, a well-characterized model of alcohol dependence and stress-induced escalation of drinking. After establishing stable baseline drinking, mice underwent four cycles of CIE or AIR with alternating weeks of alcohol drinking, and a subset underwent 10 minutes of forced swim stress 4 hours prior to each voluntary drinking session (Figure 1A). CIE mice displayed the expected increase in voluntary alcohol drinking, reaching significance in tests 3 and 4 (Fig 1B, main effect of group [$F(3,44)=19.53$, $p<0.0001$]; group x week interaction [$F(12,176)=12.12$, $p<0.0001$]; test 3, CIE vs. AIR, $p=0.0001$). This increase was enhanced when CIE mice underwent FSS prior to drinking, whereas FSS had no effect in controls (test 4, CIE vs. CIE FSS, $p<0.05$; AIR vs AIR FSS, $p=0.78$). BECs during vapor exposure did not differ between CIE and CIE+FSS

mice (Fig 1C, CIE vs. CIE FSS [F (1, 25) = 0.002456, p=0.96]). On the day of brain harvest, a subgroup of mice was sacrificed without alcohol drinking. We operationally defined this period of no alcohol access as "withdrawal," while appreciating that this term is often used to define a set of symptoms displayed by alcohol-dependent individuals. The remaining mice were given 1h of alcohol reaccess prior to sacrifice. Alcohol consumption in the subset of mice that drank on the day of sacrifice was representative of the cohort as a whole, where CIE mice drank more than AIR and AIR+FSS mice, and CIE+FSS showed further escalated drinking (significant effect of group [F (3, 44) = 34.82, p<0.0001]; CIE vs. AIR, p<0.0001; CIE vs. AIR+FSS, p=0.0001; CIE vs. CIE+FSS, p=0.004).

Alcohol withdrawal causes widespread neuronal activation in CIE mice

We then performed iDISCO whole-brain c-fos immunolabeling and clearing of hemisected brains, followed by light sheet imaging and ClearMap analysis, a well-validated method for quantifying the number of c-fos-positive cells in brain regions registered to the Allen Brain Atlas. Figure S1 shows representative images of cleared brain hemispheres from each group; Figure S2A-D shows representative images of c-fos-stained nuclei in cleared brain tissue; and Figure S2E-F shows c-fos counts from selected brain regions. A list of included brain regions and c-fos counts from individual subjects is included in Tables S1 and S2. We assessed the impact of CIE and FSS on neuronal activation during withdrawal by conducting two-way ANOVAs on raw c-fos counts for individual brain regions. Using a false discovery rate (FDR) of 5% to account for multiple comparisons, regions with raw p values <0.0063 were considered statistically significant. CIE induced widespread increases in c-fos expression, with the effect size reaching significance in 40 regions (Figure S3, main effect of CIE): lzHY, BA, PAA, SI, COA, PA, SOC, PVZ, NLOT, BST, VIS, MEA, ARH, MRN, MA, BMA, PRN, PIR, STR, PT, DORsm, AAA, CA2, PB, SPF, IA, CA3, SCm, PV, STRd, CUN, CA1, PVH, PAG, STRv, OT, ENT, SCs, PPN, and sAMY. FSS increased c-fos in SS, AUD, VIS, and SCs. While FSS tended to augment the CIE-induced increase in c-fos, no FSSxCIE interaction was detected. Statistical results, including post-hoc test results for each region, are available in Table S3.

Alcohol reaccess drinking differentially affects c-fos in high and low drinkers

A low n (n=3) in the AIR reaccess group due to a tissue processing error precluded a full group analysis for the reaccess condition. Because we detected minimal effects of FSS on c-fos counts, and correlation-based analyses are susceptible to errors driven by small sample size, we collapsed the four groups (AIR, AIR+FSS, CIE, and CIE+FSS) into two comprising high and low alcohol drinkers (HD and LD) for subsequent analyses. As individual mice exhibit daily variability in drinking, we averaged drinking values from tests 3 and 4 to compute a mean for each mouse, and those with intake above the mean (2.7 g/kg/h) were designated as HD mice (Figure 1D). Notably, the HD group comprised CIE and CIE+FSS mice, with only one CIE mouse reassigned to the LD group. Consistent with these designations, intake was significantly different and showed no overlap between LD and HD mice on the day of sacrifice (Figure 1E). We then explored the patterns of alcohol-induced c-fos activation associated with differential drinking behavior. Two-way ANOVAs were conducted on raw c-fos counts for individual brain regions, with drinking history and reaccess as the independent variables. Using an FDR of 5%, regions with raw p

values <0.0082 were considered statistically significant. There was a main effect of reaccess drinking to increase c-fos in STRd, while it decreased c-fos in SCm, SCs, VIS, and GENv (Figure 2). The effect of drinking history (HD vs. LD) was significant in 13 regions: AAA, BA, IA, STR, STRd, TEa, VIS, CLA, COA, NLOT, PAA, lzHY, PIR. In each of these regions, HD mice had higher c-fos than LD mice, driven primarily by the elevated c-fos during withdrawal. There was also a prominent interaction between drinking history and reaccess drinking. Drinking increased c-fos in LD mice but suppressed c-fos in HD mice in 34 regions: CA1, CA2, CA3, DG, BST, BA, MEA, MS, SI, VIS, BMA, PA, SPF, DORsm, CUN, MRN, PAG, PPN, RN, SCm, SNc, SNr, COA, NLOT, PAA, ARH, DMH, lzHY, mzHY, PV, PVZ, VMH, PB, and PRN (Figure 2). Post-hoc test results are included in Table S3.

Chronic alcohol and reaccess drinking reorganize functional brain networks

We next performed a network analysis to assess how alcohol history and/or reaccess drinking changed coactivation among brain regions. We built fully connected, undirected, signed, weighted networks for each treatment group, generated from between-subject interregional correlations (Figure 3A-D). The hierarchical consensus clustering (HCC) procedure revealed a nested community structure in which the networks were divisible into smaller clusters of increasingly strong interregional correlations for up to 6 levels (Figure 3E-L). This hierarchical organization was statistically above chance and consistent with observations in anatomical human and rodent networks (Jeub et al., 2018). The network communities for LD and HD mice are shown in Figures 4 and 5, respectively.

We next computed the adjusted mutual information (AMI) between the HCC community partitions and the anatomical group partitions as defined by the Allen Brain Atlas (Figure S4). AMI indicated a high degree of overlap between HCC and anatomical clusterings for all four groups. This finding is represented in Figures 4 and 5, where communities are largely composed of multiple regions from the same anatomical group. This partial correspondence between the functional communities and anatomical groups was observed in all conditions and indicates that the HCC communities may be capturing interaction patterns of coordinated regions belonging to both the same and different anatomical systems, revealing information exchange across systems.

For each network, we calculated the mean coactivation, anatomical modularity, and HCC modularity (Table 1). Whereas anatomical modularity is calculated given the anatomical groups from the Allen Brain Atlas, HCC modularity is calculated using the HCC communities. Because only a single network was generated for each condition, we statistically compared group pairs by computing the empirical difference between groups and building a null model using a permutation procedure (Table 2). Mean coactivation was not different among the groups (Table 2). However, anatomical modularity was lower in the HD withdrawal network compared to HD reaccess network, indicating that reaccess alcohol drinking increased the interactivity of intra-anatomical groups in HD mice. This effect of reaccess alcohol was not observed in LD mice. We also observed a higher HCC modularity in the HD reaccess network compared with both HD withdrawal and LD reaccess networks (Table 2). These differences are visualized in Figure 3A-D, where the HD reaccess network

has a larger number of negative correlations (shown in blue) than the HD withdrawal and LD reaccess groups, resulting in more segregated communities.

Chronic alcohol and reaccess drinking alter coactivation metrics

We aimed to identify brain regions that significantly change their interaction patterns following chronic alcohol exposure, and to understand how such changes reflect the community structure and overall change in brain state. After performing HCC and obtaining the functional communities, we computed the within-community strength (wcs) and diversity coefficient (h) for each region given its community allegiance and compared these metrics among conditions in a pairwise manner. Whereas wcs captures the strength of a region's coactivation within its assigned community, h captures the strength of its coactivation with other communities. Figure 6 shows the regions that were statistically different in these two-by-two comparisons (Fig 6A-F); statistical results are available in Table S4. Relatively few regions showed changes in wcs between conditions. The substantia innominata (SI) was significant in two comparisons; wcs was higher in HD relative to LD mice during withdrawal (Figure 6A, $p<0.05$), and reaccess drinking increased wcs of the SI in LD mice (Figure 6B, $p<0.05$). Interestingly, the SI also showed different community associations in HD and LD mice (Figures 4 and 5); in HD mice, it was part of a large, densely connected community spanning multiple anatomical groups, whereas in LD mice, regardless of reaccess alcohol drinking, it was part of a smaller cluster composed mainly of other cerebral nuclei. Thalamic regions also showed differences in wcs across conditions, although this was not specific to any one subregion. Reaccess drinking increased wcs in several thalamic subregions in LD mice (Figure 6B), but reduced wcs in thalamic subregions in HD mice (Figure 6C).

We observed a similar pattern of results for the diversity coefficient (Figure 6D-F). Diversity of many regions was higher in HD than LD mice during withdrawal (Figure 6D). Reaccess drinking had opposite effects in HD and LD mice, reducing diversity across many regions in HD mice (Figure 6F), but increasing it in LD mice (Figure 6E). To identify regions of high importance, whose diversity coefficient changed across multiple conditions, we represented the mutually significant regions in a Venn diagram (Figure 6G). We were particularly interested in regions with elevated diversity in HD mice during withdrawal that was reduced by reaccess drinking; activity in these regions could promote high levels of c-fos activation occurring across communities during the withdrawal condition, contributing to the drive to drink alcohol. Regions meeting these criteria included the DG and CA3, and three olfactory regions, COA, NLOT, and PAA, as well as the BA, an anatomically adjacent structure with vomeronasal functions (16). Interestingly, diversity of these four regions was increased by reaccess alcohol in LD mice, suggesting that acute modulation by alcohol may produce long-term changes in connectivity with repeated high-level exposure.

COA silencing reduces drinking in CIE mice

Our network analysis identified several regions with higher diversity in the HD withdrawal condition compared to LD withdrawal and HD reaccess, suggesting these regions may influence cross-community network activity during withdrawal and contribute to the heightened brain-wide activity that we suspect drives relapse drinking. We tested this

hypothesis in the COA, a chemosensory brain region that mediates olfactory influences on motivated behaviors. The COA projects densely to CeA and exhibits reciprocal connections with subcortical areas implicated in alcohol dependence (17). Using designer receptors exclusively activated by designer drugs (DREADDs) (18), we inhibited this region during an alcohol reaccess session. Mice were stereotaxically injected with an AAV expressing either hM4Di-mCherry or control virus in bilateral COA, and then underwent 4–5 weeks of baseline drinking followed by four cycles of CIE or AIR (Figure 7A, n=11–16 per group). Mice received saline injections 30 minutes prior to each drinking session beginning in test 3, reflected in a reduction in drinking in both AIR and CIE mice at this timepoint (Figure 7G). However, this reduction did not obscure the effect of CIE to increase drinking in tests 3 and 4 relative to AIR (Figure 7G). On day 3 of test 4, mice were given 3 mg/kg CNO 30 minutes prior to drinking instead of saline. Because mice exhibit substantial variability in day-to-day drinking, alcohol intake following CNO was compared to the average intake on the three surrounding days when mice received saline injections (Figure 7I). CNO reduced drinking selectively in CIE mice expressing the hM4Di virus (effect of CNO: $F(1,52) = 20.15$, $p<0.001$; effect of CIE: $F(1,52) = 9.674$, $p=0.003$; CNO x CIE interaction, $F(1,52) = 10.15$, $p=0.0024$; trend for CNO x CIE x virus interaction, ($F(1,52) = 3.807$, $p=0.056$; post-hoc Sidak's test, CIE hM4Di CNO vs. CIE hM4Di saline, $p=0.0002$, CIE mCherry CNO vs. CIE mCherry saline, $p=0.72$). To determine if reduced drinking in CIE hM4Di mice was selective to alcohol, we then assessed sucrose consumption. CNO had no effect on sucrose or water consumption or preference (Figure 7J-L), although there was a main effect of hM4Di virus to reduce sucrose consumption (3-way-ANOVA, $p=0.03$, Figure 7J). We also tested whether reduced alcohol consumption could be due to reduced locomotion; no differences in distance traveled or mean velocity were detected in a 30-minute test of locomotion 30 minutes following a CNO injection (Figure 7M,N).

Discussion

We demonstrated that acute (24h) alcohol withdrawal in high-drinking, CIE- and CIE/FSS-exposed mice produces widespread neuronal activation and changes in network community architecture marked by increased cross-module communication of multiple brain regions. Reaccess drinking suppressed this increase in neuronal activation and reversed withdrawal-induced changes in coactivation, increasing brain modularity. We identified several olfactory brain regions, including the COA, as potentially important drivers of cross-community neural activation during withdrawal. Gi-DREADD-mediated inhibition of the COA reduced voluntary drinking during withdrawal in CIE mice, validating our network approach and suggesting that the COA, and other olfactory-associated brain regions, may be novel regions of importance for alcohol dependence.

Prior studies have assessed c-fos expression following acute and chronic alcohol intake, but this is the first to assess global c-fos activation during alcohol withdrawal and following alcohol reaccess in the CIE model. We identified widespread neuronal activation during alcohol withdrawal, including in regions not previously implicated in alcohol drinking. This is consistent with alcohol-induced neuroadaptations that promote hyperexcitability, such as reduced inhibitory neurotransmission via GABAa receptors and increased excitatory glutamatergic transmission (19). Binge-level consumption in high-drinking mice suppressed

the withdrawal-induced increase in c-fos, consistent with depressant effects of alcohol at high concentrations. Similar observations were made in a recent study examining the time course of c-fos expression post CIE, albeit in a more restricted set of brain regions (20); c-fos expression was reduced during alcohol vapor-induced intoxication, but increased in most regions at 26h of withdrawal. Whereas our study captured withdrawal 24 hours post drinking rather than peak vapor withdrawal, the timing post intoxication is similar. Another study in rats exposed to CIE or self-administered alcohol vapor also showed elevated c-fos in several regions during acute withdrawal, with self-administration recruiting additional brain regions over CIE (21).

Whereas reaccess drinking suppressed c-fos in HD mice, it increased c-fos in many of the same brain areas in LD mice. This was evident in regions already implicated in drinking, such as the extended amygdala and lateral hypothalamus, as well as many understudied regions such as the substantia innominata. Studies of alcohol-induced immediate early gene expression in rodents, focusing on addiction-related brain regions, show nearly universal increases in c-fos following acute administration or voluntary consumption of 1–4 g/kg alcohol in naive animals or following short-term repeated exposure. The differential response of HD and LD mice to acute alcohol may reflect differing alcohol doses, as HD mice consumed approximately twice as much alcohol as LD mice, or it may reflect the neuroplasticity from chronic alcohol that changes its pharmacological outcome. Importantly, c-fos here may capture not only pharmacological effects of alcohol, but also neural responses associated with the experience of the test, for example, cue-induced effects, which may differ between groups. Interestingly, although LD and HD mice had different c-fos values during withdrawal, and consumed different amounts of alcohol, c-fos counts post-drinking were similar for most regions. This suggests that mice drink until reaching a homeostatic point, and allostatic mechanisms in dependent mice increase the amount of alcohol required to reach this point.

One goal of our study was to gain insight into how FSS escalates drinking in CIE mice. Four hours post FSS, there was increased activation of sensory-related systems in both AIR and CIE mice, specifically in the auditory, somatosensory, and visual cortices, and the sensory-related superior colliculus. Sensory hyperreactivity is a known consequence of acute alcohol withdrawal (22), and FSS may exacerbate this state in CIE mice. Although there was no interaction between FSS and CIE for any region, CIE+FSS mice showed a tendency toward further elevation of c-fos across the brain during withdrawal. Consistent with this, a recent whole-brain c-fos mapping study in mice found that acute stress increased c-fos in most brain regions examined, supporting the idea that stress promotes widespread increases in neuronal activation (23). This trend for increased c-fos following FSS was not observed in AIR mice, coinciding with their lack of escalation in drinking. Mice habituate to repeat stressors, including FSS (24), suggesting AIR mice may have adapted to FSS over time. CIE mice show increased corticosterone following a single FSS (25), and they may differentially adapt to repeat FSS due to alcohol dysregulation of stress systems, although this was not explicitly assessed (26). As tissue was collected four hours post stressor, differences in stress recovery between AIR and CIE may be particularly important.

When we analyzed how these global c-fos changes translated into network function changes, several patterns emerged. During withdrawal, there were no differences between LD and HD mice in general network features such as mean coactivation or modularity; however, the community configurations differed, and increased diversity in many regions in the HD withdrawal group indicates substantial coactivation with regions outside of their assigned communities. Following reaccess drinking, network properties were significantly altered in HD but not LD mice. Alcohol reaccess increased HCC modularity in HD mice, indicating increased segregation of the communities identified by HCC, and also increased anatomical modularity, indicating greater interactivity of intra-anatomical groups. Similarly, alcohol reaccess reduced diversity in many regions in HD mice, indicating lower inter-community coactivation, consistent with the increase in modularity.

A recent study examined c-fos networks after 7 days of abstinence from alcohol in CIE mice. They identified increased coordinated activity in CIE compared with nondependent and alcohol-naïve mice, and identified a cluster of extended amygdalar regions whose activity was uniquely anti-correlated with that of regions in other modules (15). In our study, HD mice were studied after only 24h of abstinence but showed a similar increase in interregional correlation (Fig. 3), suggesting this may be a long-lasting change after withdrawal from chronic high-level alcohol. However, we did not observe an anti-correlated amygdala cluster, suggesting that the extended amygdala may undergo continued remodeling over the course of abstinence. Comparison of modules and hubs identified in the two studies is difficult due to methodological differences; while the prior study employed arbitrary correlation thresholds, we used a data-driven approach and incorporated both positive and negative correlations, as the latter are important for network responsiveness (27).

Modular organization, where neural elements form strong within-module connections and weak inter-module connections, is a feature of complex networks that increases efficiency and supports specialized processing (28). We did not detect a reduction in overall brain modularity in HD mice during withdrawal, but the increase in diversity of many regions (Fig. 6D) suggests similar functional changes at the circuit level. Increased modularity in HD mice following alcohol reaccess (Table 2) was at least partly due to an increase in negative correlations (increased blue in Fig. 3D) resulting from alcohol inhibition of circuit activity. Thus, acute withdrawal in HD mice appears to produce widespread nonspecific activation of extraneous circuits, in essence increasing the noise in the system, and drinking may increase modularity by suppressing this inappropriate circuit activity. The alcohol-dependent brain may therefore function more efficiently after alcohol reaccess, contributing to the drive to consume alcohol.

Our network findings echo those of two recent human fMRI studies, where alcohol-dependent subjects showed changes in the network community structure at baseline, and relapse caused the community configuration to become more similar to that of control subjects. In one study, abstinent drinkers displayed increased global cross-community interaction of the vmPFC, particularly with the visual-cortex containing community, and this difference was reversed following relapse (29). Similarly, we observed a significantly elevated diversity coefficient in abstinent HD mice in PL, ILA, and ACA, rodent correlates

of human PFC (30); while reaccess tended to attenuate these diversity measures in high drinkers, this finding did not reach significance. In another human imaging study, basal ganglia and thalamic nodes had different community associations in heavy drinkers compared to controls during abstinence, and returned to similar configurations as controls following relapse (31). However, modularity was not different in drinkers relative to controls either before or after relapse. These two studies suggest that in alcohol-dependent human subjects, drinking normalizes aspects of network function that have likely been disrupted by chronic alcohol use. Similarly, in HD mice, drinking reduces some of the network disruptions observed during withdrawal, making the community configuration more similar to that of LD mice during withdrawal.

Network analysis pointed to a cluster of anatomically adjacent olfactory brain regions that may be particularly susceptible to modulation by both chronic alcohol and reaccess drinking. These included the COA, PAA, NLOT, and BA, which showed increased c-fos activation after reaccess alcohol in LD mice, and increased c-fos during withdrawal in HD mice that was reversed by reaccess drinking. Similar patterns were observed for network diversity coefficients. One possible explanation is that chronic alcohol vapor inhalation damages peripheral olfactory pathways. While not studied in the CIE model, evidence in rodents indicates that acute alcohol inhalation causes olfactory neuronal death, as well as retrograde changes in the hippocampus, another high-diversity region in our study. However, alcohol-induced olfactory changes are not specific to the vapor route of administration. Chronic alcohol drinking causes olfactory damage in both humans and rodents (32–34). In humans, alcohol has acute dose-dependent effects on olfaction, where low-dose drinking increases olfactory perception, and high-dose drinking blunts olfaction (35). Thus, alcohol can both acutely alter olfaction and lead to chronic changes in olfactory brain regions over time, even when consumed orally. Our DREADD experiment supports the role of cortical amygdala in withdrawal-induced drinking, and the other olfactory regions identified are predicted to have similar effects. Interestingly, chronic stress also causes significant olfactory dysfunction in rodents, mediated in part by changes in the NLOT (36), suggesting that the olfactory cluster we identified may be an important locus for stress-alcohol interactions.

A key limitation of this study is the use of the collapsed dataset for the network analysis, which precluded assessing the effects of FSS on network properties in CIE mice. CIE and CIE+FSS mice showed significant differences in drinking behavior, and c-fos counts tended to be higher in the latter. It is unknown if this would translate into an exacerbation of the observed network changes in CIE+FSS mice (e.g., further reduced modularity), or if distinct networks would emerge. However, it is reassuring that a high-centrality target region identified using the collapsed dataset was validated in a CIE cohort that did not undergo FSS. Another limitation is the use of only male mice. Although FSS was not incorporated as a variable in our network analysis, we were initially interested in FSS-induced escalation, and we omitted females because they do not show this phenotype (37). Examining the networks associated with alcohol dependence in females is a key area for followup studies. A more general limitation is the use of c-fos as a proxy for neuronal activity. Neuronal activation can be independent of immediate-early-gene induction under conditions of chronic activation or net synaptic inhibition (38), and there are instances of glial c-fos induction in neuroinflammatory states (39). That our c-fos measures are in agreement

with other indicators of neuronal excitability during withdrawal (electrophysiological, etc.) suggests a neuronal component; given the neurotoxic and inflammatory effects of alcohol, a glial contribution is also possible. Global and regional exploration of specific cell types remains an important area for future study.

Supplementary Material

Refer to Web version on PubMed Central for supplementary material.

Acknowledgements

This work was supported by the National Institutes of Health (NIH) National Institute of Alcohol Abuse and Alcoholism (NIAAA) grant 2U01AA020911–11 to T.L.K., and National Institute of Mental Health (NIMH) R01MH119421 and funding from the Liquor Control Board of Ontario (LCBO) to P.W.F. Some figures for this manuscript were created using BioRender.com. We thank Pablo Ariel, Ph.D. and the UNC Microscopy Sevices Laboratory for assistance with lightsheet imaging. The Microscopy Services Laboratory, Department of Pathology and Laboratory Medicine, is supported in part by P30 CA016086 Cancer Center Core Support Grant to the UNC Lineberger Comprehensive Cancer Center. Research reported in this publication was supported in part by the North Carolina Biotech Center Institutional Support Grant 2016-IDG-1016.

References

1. Heilig M, Koob GF (2007): A key role for corticotropin-releasing factor in alcohol dependence. Trends Neurosci 30: 399–406. [PubMed: 17629579]
2. Koob GF (2008): A Role for Brain Stress Systems in Addiction. Neuron 59: 11–34. [PubMed: 18614026]
3. Becker HC (2013): Animal models of excessive alcohol consumption in rodents. Curr Top Behav Neurosci 13: 355–377. [PubMed: 22371267]
4. Metten P, Sorensen ML, Cameron AJ, Yu C-H, Crabbe JC (2010): Withdrawal severity after chronic intermittent ethanol in inbred mouse strains. Alcohol Clin Exp Res 34: 1552–1564. [PubMed: 20586758]
5. Logan RW, Seggio JA, Robinson SL, Richard GR, Rosenwasser AM (2010): Circadian wheel-running activity during withdrawal from chronic intermittent ethanol exposure in mice. Alcohol Fayettev N 44: 239–244.
6. Sidhu H, Kreifeldt M, Contet C (2018): Affective Disturbances During Withdrawal from Chronic Intermittent Ethanol Inhalation in C57BL/6J and DBA/2J Male Mice. Alcohol Clin Exp Res 42: 1281–1290. [PubMed: 29687895]
7. Becker HC, Lopez MF (2004): Increased ethanol drinking after repeated chronic ethanol exposure and withdrawal experience in C57BL/6 mice. Alcohol Clin Exp Res 28: 1829–1838. [PubMed: 15608599]
8. Griffin WC, Lopez MF, Yanke AB, Middaugh LD, Becker HC (2009): Repeated cycles of chronic intermittent ethanol exposure in mice increases voluntary ethanol drinking and ethanol concentrations in the nucleus accumbens. Psychopharmacology (Berl) 201: 569–580. [PubMed: 18791704]
9. Anderson RI, Lopez MF, Becker HC (2016): Forced swim stress increases ethanol consumption in C57BL/6J mice with a history of chronic intermittent ethanol exposure. Psychopharmacology (Berl) 233: 2035–2043. [PubMed: 26935824]
10. Haun HL, Lebonville CL, Solomon MG, Griffin WC, Lopez MF, Becker HC (2022): Dynorphin/Kappa Opioid Receptor Activity Within the Extended Amygdala Contributes to Stress-Enhanced Alcohol Drinking in Mice. Biol Psychiatry 91: 1019–1028. [PubMed: 35190188]
11. Lopez MF, Anderson RI, Becker HC (2016): Effect of different stressors on voluntary ethanol intake in ethanol-dependent and nondependent C57BL/6J mice. Alcohol Fayettev N 51: 17–23.

12. Simpson S, Chen Y, Wellmeyer E, Smith LC, Aragon Montes B, George O, Kimbrough A (2021): The Hidden Brain: Uncovering Previously Overlooked Brain Regions by Employing Novel Preclinical Unbiased Network Approaches. Front Syst Neurosci 15: 595507. [PubMed: 33967705]
13. Smith LC, Kimbrough A (2020): Leveraging Neural Networks in Preclinical Alcohol Research. Brain Sci 10: E578.
14. Wheeler AL, Teixeira CM, Wang AH, Xiong X, Kovacevic N, Lerch JP, et al. (2013): Identification of a functional connectome for long-term fear memory in mice. PLoS Comput Biol 9: e1002853. [PubMed: 23300432]
15. Kimbrough A, Lurie DJ, Collazo A, Kreifeldt M, Sidhu H, Macedo GC, et al. (2020): Brain-wide functional architecture remodeling by alcohol dependence and abstinence. Proc Natl Acad Sci U S A 117: 2149–2159. [PubMed: 31937658]
16. Kevetter GA, Winans SS (1981): Connections of the corticomedial amygdala in the golden hamster. I. Efferents of the “vomeronasal amygdala.” J Comp Neurol 197: 81–98. [PubMed: 6164702]
17. Cádiz-Moretti B, Abellán-Álvaro M, Pardo-Bellver C, Martínez-García F, Lanuza E (2017): Afferent and efferent projections of the anterior cortical amygdaloid nucleus in the mouse. J Comp Neurol 525: 2929–2954. [PubMed: 28543083]
18. Armbruster BN, Li X, Pausch MH, Herlitze S, Roth BL (2007): Evolving the lock to fit the key to create a family of G protein-coupled receptors potently activated by an inert ligand. Proc Natl Acad Sci U S A 104: 5163–5168. [PubMed: 17360345]
19. Becker HC, Mulholland PJ (2014): Neurochemical mechanisms of alcohol withdrawal. Handbook of Clinical Neurology, vol. 125. Elsevier, pp 133–156. [PubMed: 25307573]
20. Smith RJ, Anderson RI, Haun HL, Mulholland PJ, Griffin WC, Lopez MF, Becker HC (2020): Dynamic c-Fos changes in mouse brain during acute and protracted withdrawal from chronic intermittent ethanol exposure and relapse drinking. Addict Biol 25: e12804. [PubMed: 31288295]
21. de Guglielmo G, Simpson S, Kimbrough A, Conlisk D, Baker R, Cantor M, et al. (2023): Voluntary and forced exposure to ethanol vapor produces similar escalation of alcohol drinking but differential recruitment of brain regions related to stress, habit, and reward in male rats. Neuropharmacology 222: 109309. [PubMed: 36334765]
22. Becker HC (2000): Animal Models of Alcohol Withdrawal. Alcohol Res Health 24: 105. [PubMed: 11199277]
23. Azevedo H, Ferreira M, Mascarello A, Osten P, Guimarães CRW (2020): Brain-wide mapping of c-fos expression in the single prolonged stress model and the effects of pretreatment with ACH-000029 or prazosin. Neurobiol Stress 13: 100226. [PubMed: 32478146]
24. Lovelock DF, Deak T (2017): Repeated exposure to two stressors in sequence demonstrates that corticosterone and paraventricular nucleus of the hypothalamus interleukin-1β responses habituate independently. J Neuroendocrinol 29. 10.1111/jne.12514
25. Maldonado-Devincci AM, Kampov-Polevoi A, McKinley RE, Morrow DH, O’Buckley TK, Morrow AL (2016): Chronic Intermittent Ethanol Exposure Alters Stress Effects on (3α,5α)-3-hydroxy-pregnan-20-one (3α,5α-THP) Immunolabeling of Amygdala Neurons in C57BL/6J Mice. Front Cell Neurosci 10: 40. [PubMed: 26973459]
26. Retson TA, Sterling RC, Bockstaele EJV (2016): Alcohol-induced dysregulation of stress-related circuitry: the search for novel targets and implications for interventions across the sexes. Prog Neuropsychopharmacol Biol Psychiatry 65: 252. [PubMed: 26006055]
27. Moretti J, Terstege DJ, Poh EZ, Epp JR, Rodger J (2022): Low intensity repetitive transcranial magnetic stimulation modulates brain-wide functional connectivity to promote anti-correlated c-Fos expression. Sci Rep 12: 20571. [PubMed: 36446821]
28. Zamani Esfahlani F, Jo Y, Puxeddu MG, Merritt H, Tanner JC, Greenwell S, et al. (2021): Modularity maximization as a flexible and generic framework for brain network exploratory analysis. NeuroImage 244: 118607. [PubMed: 34607022]
29. Muller AM, Meyerhoff DJ (2020): Does an Over-Connected Visual Cortex Undermine Efforts to Stay Sober After Treatment for Alcohol Use Disorder? Front Psychiatry 11: 536706. [PubMed: 33362591]

30. Laubach M, Amarante LM, Swanson K, White SR (2018): What, If Anything, Is Rodent Prefrontal Cortex? eNeuro 5. 10.1523/ENEURO.0315-18.2018

31. Muller AM, Meyerhoff DJ (2021): Maladaptive brain organization at 1 month into abstinence as an indicator for future relapse in patients with alcohol use disorder. Eur J Neurosci 53: 2923–2938. [PubMed: 33630358]

32. Collins MA, Corso TD, Neafsey EJ (1996): Neuronal degeneration in rat cerebrocortical and olfactory regions during subchronic "binge" intoxication with ethanol: possible explanation for olfactory deficits in alcoholics. Alcohol Clin Exp Res 20: 284–292. [PubMed: 8730219]

33. Obernier JA, White AM, Swartzwelder HS, Crews FT (2002): Cognitive deficits and CNS damage after a 4-day binge ethanol exposure in rats. Pharmacol Biochem Behav 72: 521–532. [PubMed: 12175448]

34. Rupp CI, Kurz M, Kemmler G, Mair D, Hausmann A, Hinterhuber H, Fleischhacker WW (2003): Reduced olfactory sensitivity, discrimination, and identification in patients with alcohol dependence. Alcohol Clin Exp Res 27: 432–439. [PubMed: 12658108]

35. Endevelt-Shapira Y, Shushan S, Roth Y, Sobel N (2014): Disinhibition of olfaction: Human olfactory performance improves following low levels of alcohol. Behav Brain Res 272: 66–74. [PubMed: 24973535]

36. Vaz RP, Cardoso A, Serrão P, Pereira PA, Madeira MD (2018): Chronic stress leads to long-lasting deficits in olfactory-guided behaviors, and to neuroplastic changes in the nucleus of the lateral olfactory tract. Horm Behav 98: 130–144. [PubMed: 29277699]

37. den Hartog CR, Blandino KL, Nash ML, Sjogren ER, Grampetro MA, Moorman DE, Vazey EM (2020): Noradrenergic tone mediates marble burying behavior after chronic stress and ethanol. Psychopharmacology (Berl) 237: 3021–3031. [PubMed: 32588079]

38. Kovács KJ (2008): Measurement of immediate-early gene activation- c-fos and beyond. J Neuroendocrinol 20: 665–672. [PubMed: 18601687]

39. Cruz-Mendoza F, Jauregui-Huerta F, Aguilar-Delgadillo A, García-Estrada J, Luquin S (2022): Immediate Early Gene c-fos in the Brain: Focus on Glial Cells. Brain Sci 12: 687. [PubMed: 35741573]

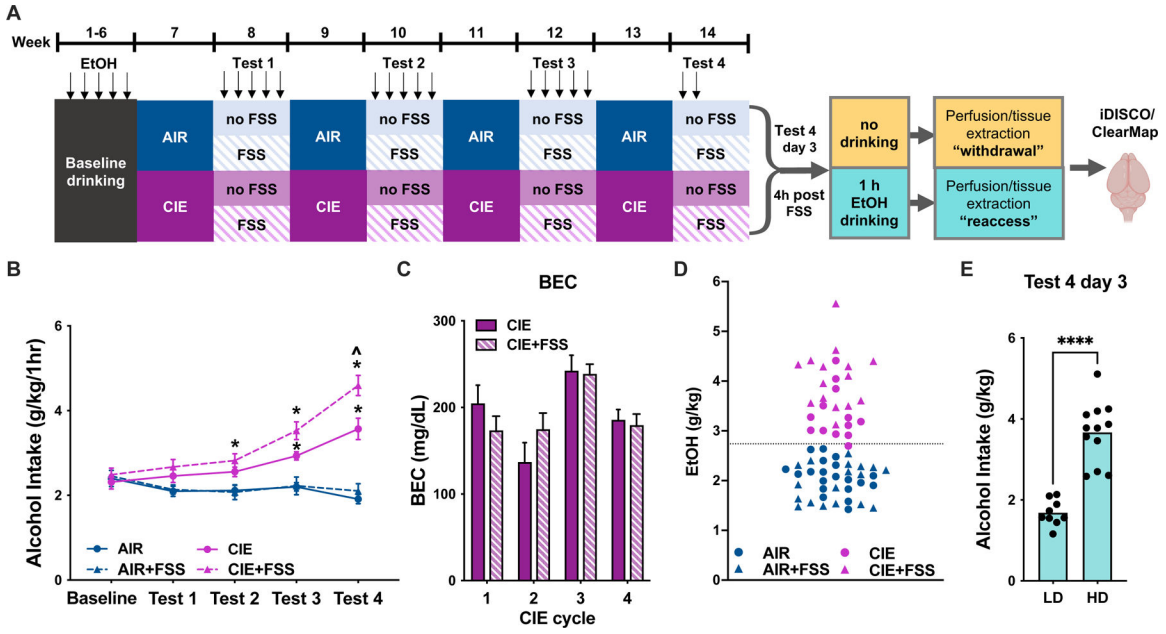

Figure 1.

A, Timeline of chronic intermittent ethanol (CIE) and forced swim stress (FSS) treatment. Following 6 weeks of baseline drinking with 15% EtOH for 1h daily, mice underwent four cycles of AIR/CIE. On alternating weeks, mice had 1h daily access to alcohol. A subset of CIE and AIR mice underwent FSS 4h prior to each drinking session. On day 3 of test 4, a subset of mice in each group was sacrificed during withdrawal, with the remaining sacrificed following a 1h drinking session ("reaccess"). B, CIE mice increased their voluntary alcohol intake across the four alcohol vapor exposure cycles. FSS further escalated drinking in CIE but not AIR mice (*, $p<0.05$ vs. AIR; ^, $p<0.05$ vs. CIE). C, Blood ethanol concentrations (BEC) during the four alcohol vapor exposure weeks. BECs did not differ between CIE and CIE+FSS mice ($p>0.05$). D, For network analysis, mice were divided into groups of low and high drinkers (LD and HD, respectively) based on intake below or above the mean of 2.7 g/kg averaged across tests 3 and 4, indicated by the dotted gray line. Only one CIE mouse showed consumption below this cutoff. E, During the final reaccess drinking session, alcohol intake was significantly higher in HD vs. LD mice ($p<0.0001$).

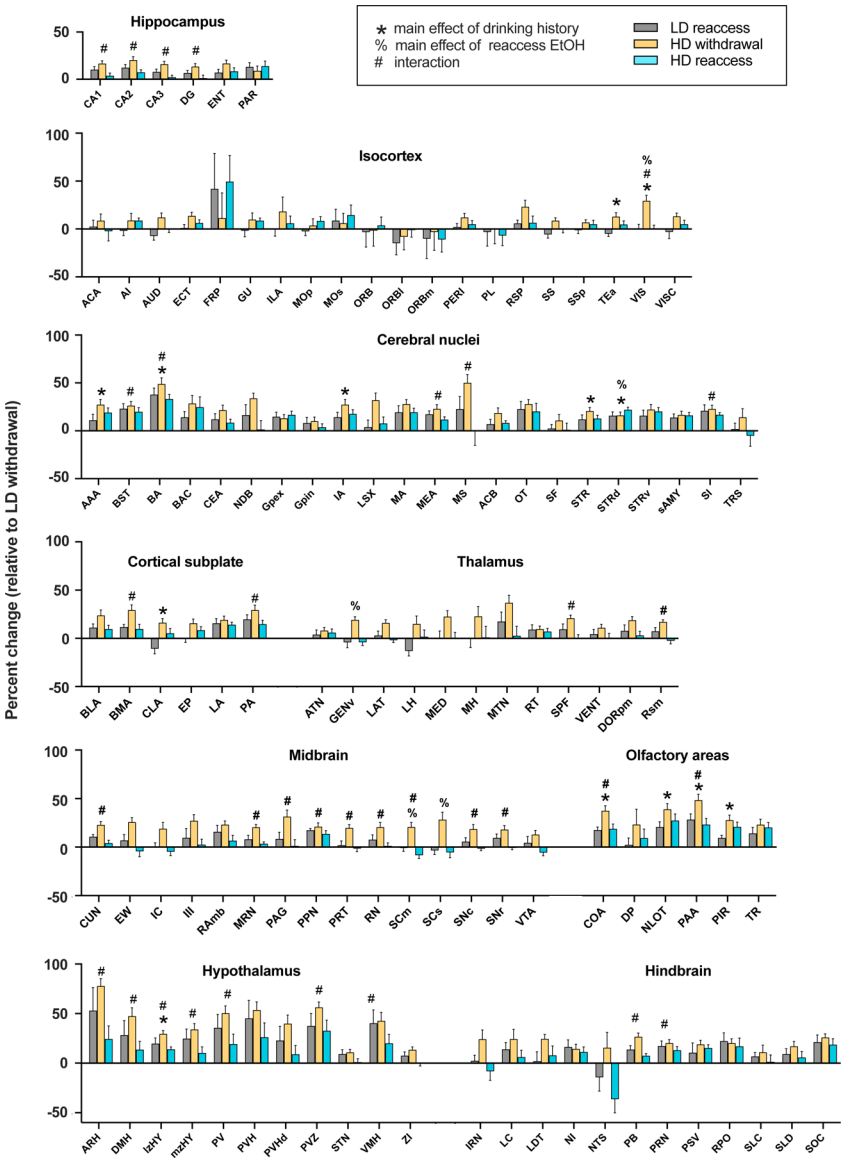

Figure 2.

A, Relative c-fos expression in high- (HD) and low-drinking (LD) mice during acute (24h) alcohol withdrawal and following a 1h alcohol reaccess period. C-fos-positive cell counts for each region are represented as the percent change relative to LD mice during withdrawal. Regions are grouped by anatomical subdivision according to the Allen Brain Atlas. * denotes a significant main effect of drinking history; % denotes a significant main effect of reaccess EtOH drinking; and # denotes a significant interaction between drinking history and alcohol reaccess (2-way ANOVA with FDR correction for multiple comparisons). Post-hoc test p-values are available in Table S3.

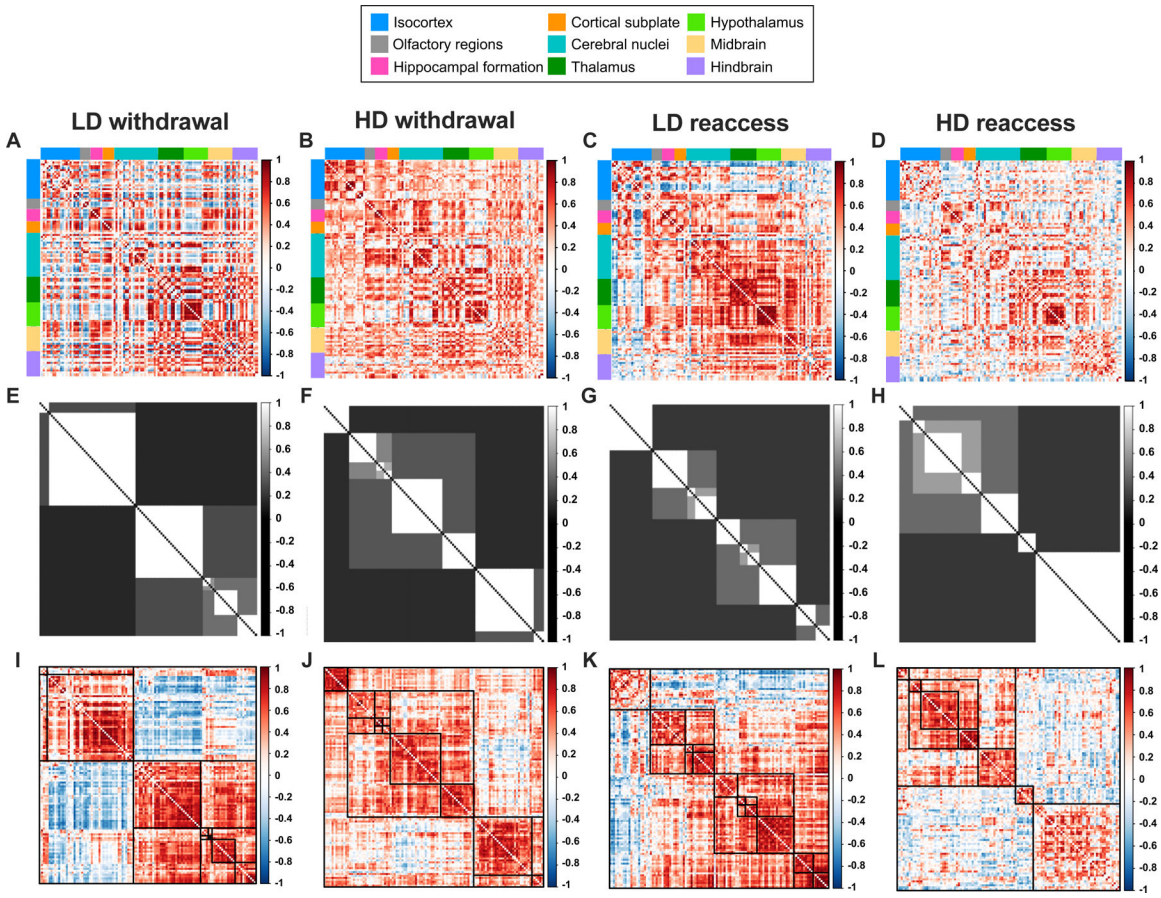

Figure 3.

A-D, Pearson correlation matrices showing interregional correlations for the 110 brain regions included in the network analysis for low-drinking (LD) and high-drinking (HD) mice during alcohol withdrawal and following alcohol reaccess. Regions are grouped by anatomical division according to the Allen Brain Atlas. E-H, Hierarchical consensus clustering (HCC) plots illustrating the community partitions of highly correlated regions. I-L, Correlation matrices derived from the HCC procedure illustrating the clustering of strongly correlated regions, denoted by darker shades of red.

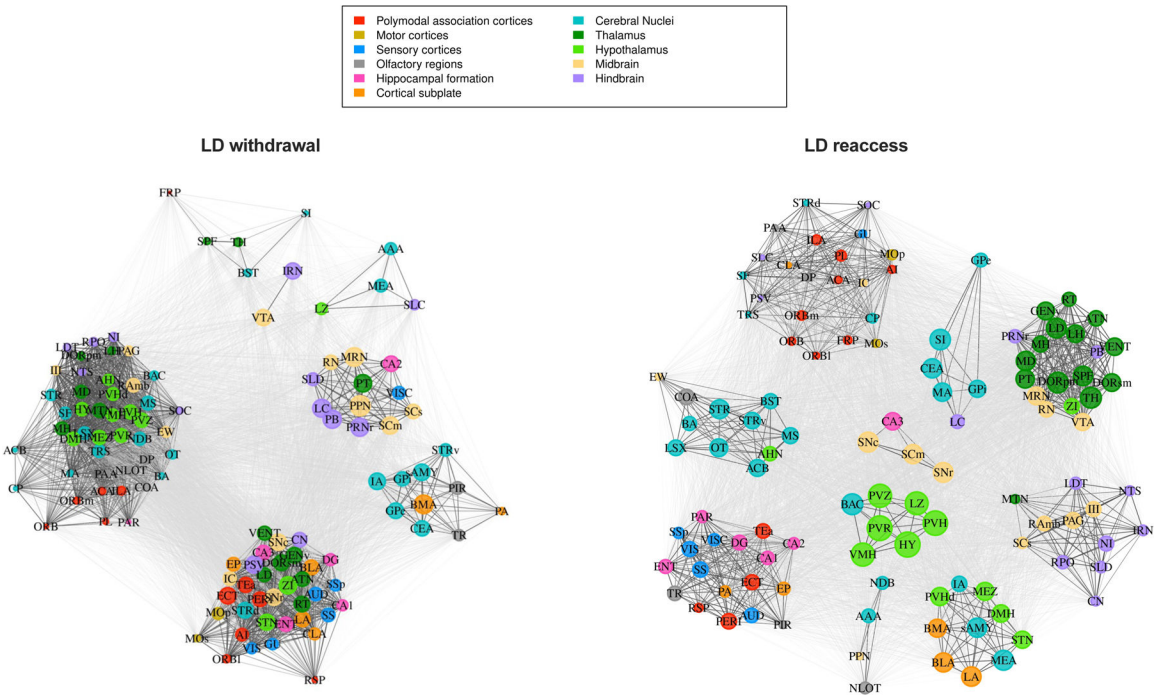

Figure 4.

Network communities for low-drinking (LD) mice in the withdrawal and reaccess conditions. Regions are color-coded according to anatomical groups defined by the Allen Brain Atlas. The size of each node in a community represents the within-community strength, whereas the strength of individual connections is represented by the edge length, i.e., the distance between nodes.

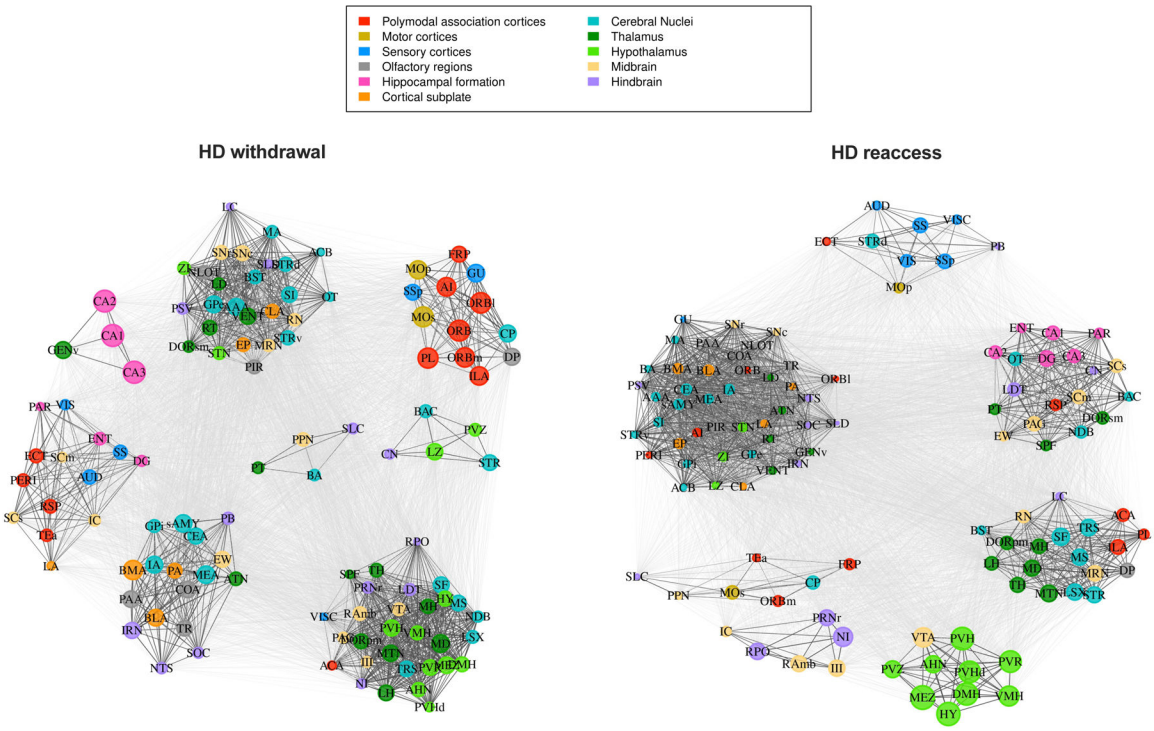

Figure 5.

Network communities for high-drinking (HD) mice in the withdrawal and reaccess conditions. Regions are color-coded according to anatomical groups defined by the Allen Brain Atlas. The size of each node in a community represents the within-community strength, whereas the strength of individual connections is represented by the edge length, i.e., the distance between nodes.

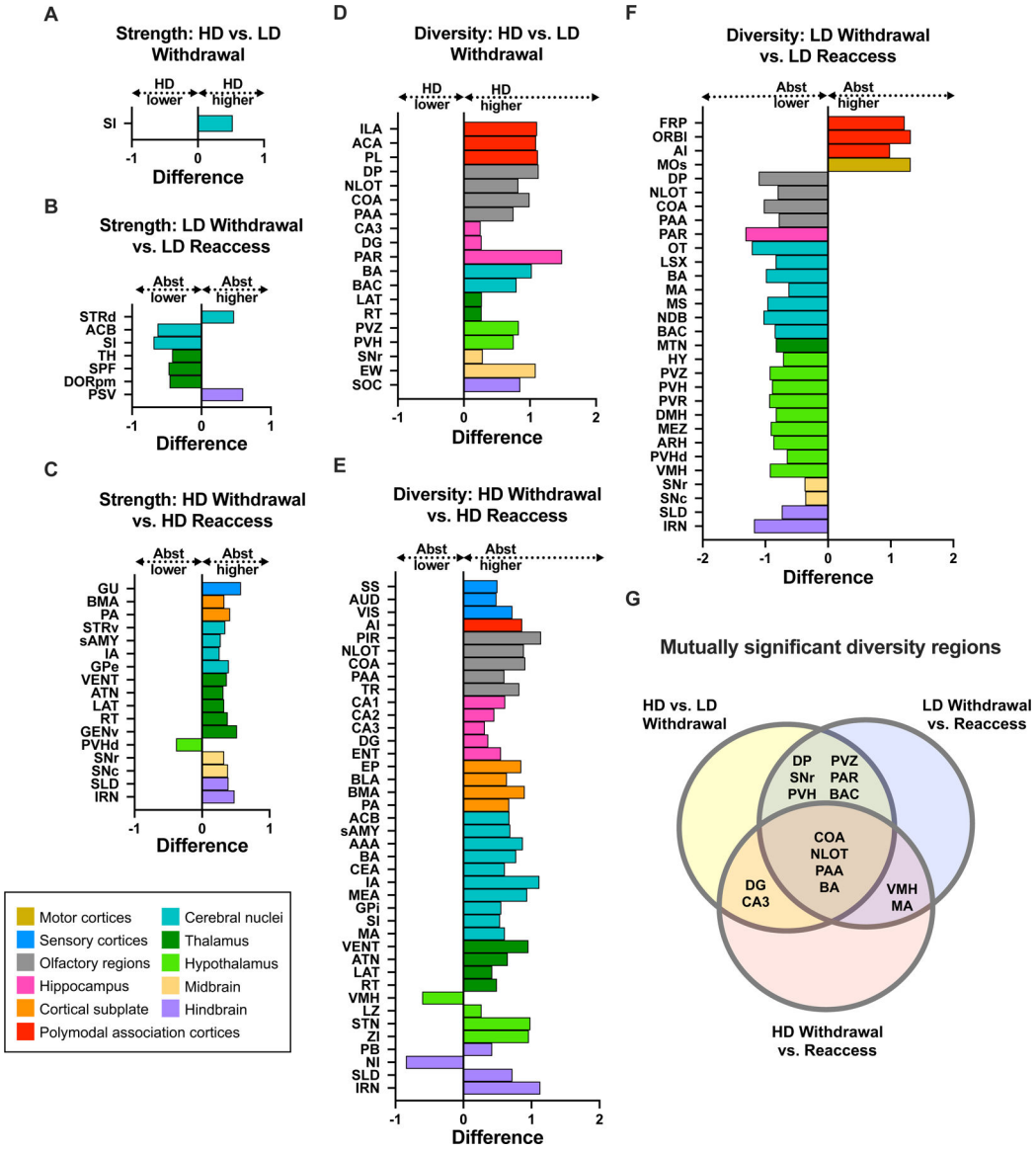

Figure 6.

Significantly different brain regions for within-community strength and diversity coefficient comparisons. A-C, Differences in within-community strength between high drinkers (HD) and low drinkers (LD) during withdrawal (A), LD withdrawal and reaccess (B), and HD withdrawal and reaccess (C). D-F, Differences in regional diversity coefficients between HD and LD withdrawal (D), HD withdrawal and reaccess (E), and LD withdrawal and reaccess (F). G, Regions with significantly different diversity coefficients shared across multiple 2-condition comparisons. A complete list of p values is available in Table S5.

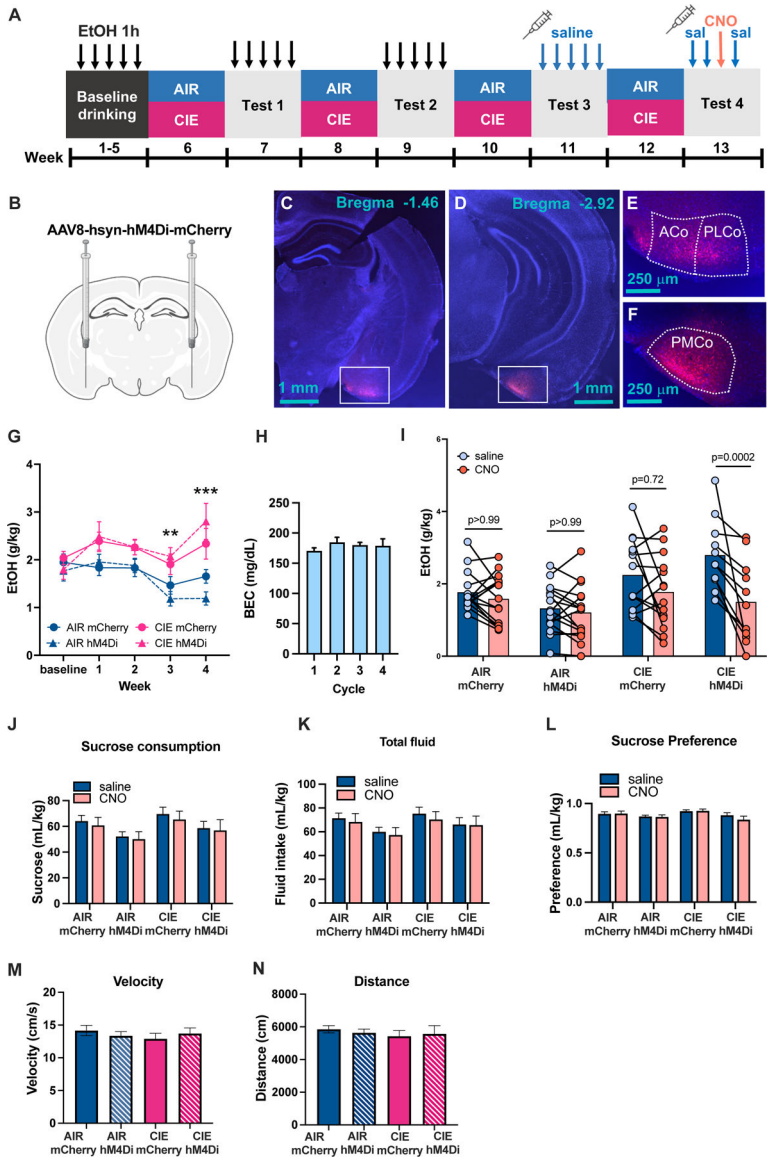

Figure 7.

A, Experimental Timeline. Following 5 weeks of baseline drinking of 15% EtOH daily for 1h, mice underwent 4 cycles of AIR/CIE vapor with alternating weeks of daily 1h alcohol access. During drinking tests 3 and 4, mice received daily saline injections 30 min prior to drinking. On day 3 of test 4, mice were injected with 3 mg/kg CNO instead of saline. B, Viral injection schematic. C-F, Representative images of viral placements in cortical amygdala showing a subject with anterior placement (C,E) and a subject with posterior placement (D,F). G, Alcohol intake was higher in CIE than AIR mice during test weeks 3 and 4, with no effect of mCherry vs. hM4Di genotype. H, BECs were relatively stable in CIE mice across the four vapor exposure weeks. I, CNO reduced drinking selectively in CIE mice expressing hM4Di virus. J-L, Sucrose consumption (J), total fluid consumption (K), and sucrose preference (L) were unaffected by CNO ($p>0.05$). We detected a main effect of hM4Di virus to reduce sucrose drinking independent of CIE or CNO treatment ($p<0.05$).

M-N, Locomotor activity measured via distance traveled (M) and mean velocity (N) did not differ based on virus or CIE exposure after CNO administration ($p>0.05$).

Table 1:

Global network metrics.

Group	Mean Coactivation	Anatomical Modularity	HCC Modularity
HD withdrawal	0.2888	0.0341	0.1723
HD reaccess	0.1101	0.0829	0.2843
LD withdrawal	0.1508	0.0496	0.3698
LD reaccess	0.2328	0.681	0.1518

Table 2:

Comparison of global level metrics among all four groups, two by two.

Comparisons	Mean Coactivation		Anatomical Modularity		HCC Modularity	
	Estimate	p value	Estimate	p value	Estimate	p value
HD withdrawal vs. HD reaccess	0.179	0.1815	**0.049**	**0.0366**	**0.112**	**0.0502**
HD withdrawal vs. LD withdrawal	0.138	0.3002	0.015	0.5205	0.1975	0.1241
HD reaccess vs. LD reaccess	0.123	0.4233	0.015	0.5555	**0.1325**	**0.0116**
LD withdrawal vs. LD reaccess	0.082	0.586	0.019	0.4539	0.218	0.166

Bold cells indicate significant differences at the significance level of $\alpha = 0.05$

KEY RESOURCES TABLE

Resource Type	Specific Reagent or Resource	Source or Reference	Identifiers	Additional Information
Add additional rows as needed for each resource type	Include species and sex when applicable.	Include name of manufacturer, company, repository, individual, or research lab. Include PMID or DOI for references; use “this paper” if new.	Include catalog numbers, stock numbers, database IDs or accession numbers, and/or RRIDs. RRIDs are highly encouraged; search for RRIDs at https://scicrunch.org/resources.	Include any additional information or notes if necessary.
Antibody	Rabbit anti-cFos	Synaptic Systems	#226–003	
Antibody	donkey anti-rabbit Alexa Fluor 647	Thermo Fisher Scientific	#A-31573	
Chemical Compound or Drug	dichloromethane	Sigma	270997	
Chemical Compound or Drug	dibenzyl ether	Sigma	108014	
Software; Algorithm	R 4.0.2	R Core Team		
Deposited Data; Public Database	Brain Connectivity Toolbox	https://sites.google.com/site/bctnet/		
Deposited Data; Public Database	R Tools for Network Analysis	https://github.com/coelhocao/Brain_Network_analysis		